FRACTURE MECHANICS APPLICATIONS FOR SPACE STRUCTURES WITHIN ESA PROGRAMS

M.Windisch

MT Aerospace AG
Franz Josef Strauß Str. 5, 86153 Augsburg
E-Mail: Michael.Windisch@mt-aerospace.de

ABSTRACT

This paper gives a short overview about the current practie of fracture mechanics methods for critical space structures as for example pressure vessels and propellant tanks. The currently applied fracture control procedures are more or less linked to the basic principles evaluated within past US space programs and reference is given to these. Special emphasis is given to non-linera fracture mechanics methods, which are applied at MT Aerospce since 20 years within European space programs as ARIANE 5 and ATV.

KEY WORDS: fracture mechanics, space applications, ESACRACK, ARIANE 5, ATV, SINTAP, damage mechanics.

1. INTRODUCTION

The development of fracture mechanics concepts and applications were strongly linked to aerospace development starting already with the Apollo program. The basic principles were first evaluated on the basis of LEFM at those days and have been continously improved up today, where non-linear methods are applied for high loaded structures where small scale yielding conditions are violated.

These improved methods as for example 3D crack simulation (j-integral) and damage mechanics material modelling allow the fracture analysis, where in the past structural tests had to be performed with large effort. In addition these methods have supported the analysis and understanding of bi-axiality and constraint effects. These effects explain the differences between the fracture behaviour of laboratory specimens and full scale structures.

2. FRACTURE MECHANICS HISTORY IN SPACE APPLICATIONS

First fundamental fracture control concepts have been evaluated which were later further specified for the space shuttle program [1,2,3,4]. These concepts include not only static fracture prediction but all aspects of the interdisciplinary nature of failure prediction as for example

- static loading (crack initiation and instability)
- cyclic loading (crack growth prediction)
- sustained loading (stress corrosion cracking and hydrogen embrittlement)
- material selection aspects

The further development of these concepts was related to a number of failure cases, which revealed the necessity of improved methods especially with the manned space programs, where failure always is linked with the loss of human life.

3. FRACTURE CONTROL

Although different space programs show slightly different approaches in fracture control principles, the main methodology is comparable. The different space programs apply own fracture control requirements. The latest ESA requirements applicable for ESA payloads and satellites can be found in [5]. The following different fracture control approaches mainly apply according to the following definitions:

Safe life: It must be demonstrated, that a crack does not become critical after application of 4 times the dimension life spectrum and always applies to single load path structures. A crack growth analysis is required.

Fail safe: Fail safe applies to multiple load path structures, where it can be demonstrated, that the loss of one load path does not lead to the failure of the remaining load paths. Limit load capability and a fatigue analysis of the remaining load paths after load redistribution is required.

Contained: A specific requirement mainly coming from the space shuttle program requires, that all potential structure elements with mass larger than g, which might be released by fatigue etc. must be contained to protect the environment from a possible impact.

LBB: For pressure vessels with non hazardous media it may be sufficient in specific cases, that a growth of an initial surface crack up to penetration will not lead to the burst of the tank but to the release of pressure by leak only.

4. GENERAL REQUIREMENTS

The damage tolerance assesment is strongly linked to the general requirements and safety factors. The yield

and ultimate load safety factors for pressurized structures are defined for structural tanks as the booster cases and the large main and upper stae cryogenic tanks and for small and high pressurant tanks as follows.

Table 1: Safety Factors

Structure	Yield	Ultimate
Structural Tanks	1.10	1.25
Propellant and High Pressurant Tanks	1.25	1.50

The minimum required burst pressure = ultimate factor x operational pressure. The same procedure applies for proof testing applying the yield safety factor. The highly mass optimized tank structures therefore at hot spots show stresses close to yield stress during proof testing and close to ultimate stress at ultimate load conditions.

The material allowables, used for the assessment, are statistical evaluated minimum properties (A-values). In the case of fracture toughess, where either large scatter is observed or only limitd tests have been performed, a knock down factor of 70% is applied on mean values, as statistics are not applicable.

A further important requirement applies for defects, which are observed during the series production. These, in most programs, have to be demonstrated against ultimate load condition.

Therefore the following two limiting cases occur in spacecraft damage tolerance assessment:

1. At hot spots local yielding may occur during proof testing. Therefore the required NDI detection limit has to be evaluated with non-linear prediction methods.
2. If a possible defects is observed (pore line in welds, inclusion in large forgings etc.), which is recharacterized as a crack, and treated with fracture mechanics, stresses for ultimate load conditions (beyond yield stress limit) have to be applied for the justification again requiring non-linear methods.

4. CURRENT PRACTICE IN EUROPEAN SPACE PROGRAMS

The application of fracture mechanics in the past US programs was limited to LEFM conditions. In those cases where the applicability of LEFM was violated, assessment was made by testing. Autofrettage of composite overwrapped pressure vessels (COPV) is a typical example. During Autofrettage large plasticity occurs and failure prediction based on LEFM does not apply.

The development of the ARIANE 5 launcher and the ATV (Automated Transfer Vehicle) spacecraft was initiated with high challenges in mass saving. The result of these goals show highly optimized structures with stresses during operational conditions close to or even at yield stress level. LEFM is applied for all low loaded structures and structural parts. ESACRACK with the module NASGRO from the US space program is applied as standard software for those parts.

Apart these, non-linear methods as R6, SINTAP, FITNET are applied [6,7,8] or even damage mechanics simulations have been used to analyze complex structural conditions [9,10,11,12]. Some examples are given in the next sections.

4.1. ARIANE 5 Booster Case Weld Interface

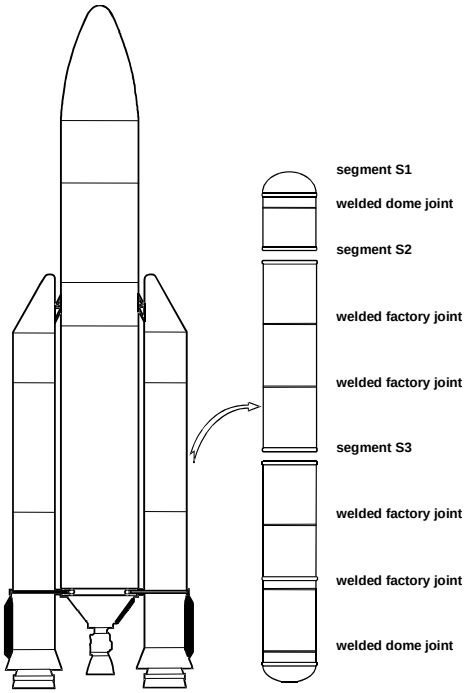

Figure 1: Schematic Illustration of ARIANE 5 Inter-Segment Connections replaced by Welds

The ARIANE 5 booster cases are made from the high strength low alloy steel 48 CrMoNiV 4 10 (D6AC) with martensitic microstructure. The relatively high carbon content (0.45 - 0.5 %) leads to high strength. The generic version consists of 8 shear bolt cnnections, which connect the 7 cylinders and two domes. The Figure 1 shows thos connections, which now have been replaced by EB welds. The EB welding is applied by one nominal weld and two cosmetic passes at the inner and outer surface, resulting in complex microstructural zones as indicated in Figure 2 and Table 2.

These different zones have all be characterized by tensile and fracture toughness tests to identify the most critical zone. In those cases, where the material zone is too small for specimen manufacturing, the material was produced by simulation of the relevant temperature vs. time cycles with a Gleeble 2000 machine

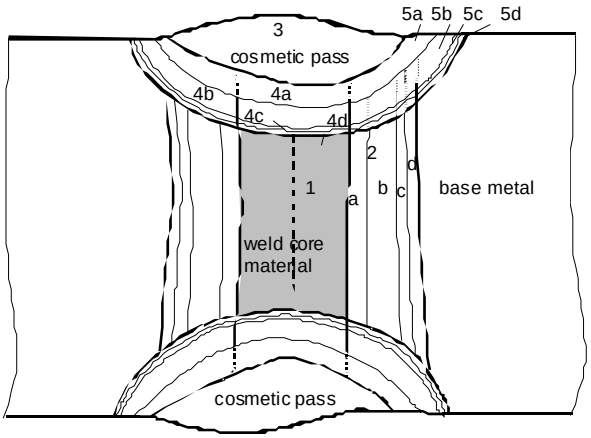

Figure 2: Definition of Microstructural Zones

Table 2: Defintion of Microstructural Zones

1	Core Weld Metal (CWM), width ≈ 3.2 mm
2	HAZ caused by the core weld: 2a = Coarse-Grained HAZ (CGHAZ), width ≈ 0.5 mm 2b = Fine-Grained HAZ (FGHAZ), width ≈ 1.65 mm 2c = Inter-critically reheated HAZ (ICHAZ), width ≈ 0.25 mm 2d = Sub-critically reheated HAZ (SCHAZ), width ≈ 0.25 mm
3	Cosmetic Pass Weld Metal (CPWM)
4	Reheated Core Weld Metal (RCWM): 4a = completely transformed CWM with austenite grain growth Globular CWM (GCWM), width ≈ 0.5 mm 4b = completely transformed CWM without austenite grain growth 4c = partially transformed (inter-critically reheated) CWM 4d = (high) Tempered CWM (TCWM), width ≈ 0.15 mm
5	HAZ caused by the cosmetic pass: 5a,b,c,d (equivalent. to 2a,b,c,d)

The before mentioned high carbon content is also responsible for brittle zones in the weld microstructure. The cleavage fracture modelling was performed on basis of the RKR model [13].

First the critical fracture stress was evaluated with the numerical simulation of notched round tensile tests as shown in Figure 3 and Figure 4. In the next step fracture toughness tests with SE(B) specimens were simulated to determine the critical distance x_c as shown in Figure 5. These two parameters are necessary for the RKR damage model. The advantage of the model is already demonstrated in Figure 5. The two specimens with different a/W ratio give different fracture toughness values but can both well be predicted with the RKR model. The well known geometry influence of fracture toughness testing is avoided with the RKR model.

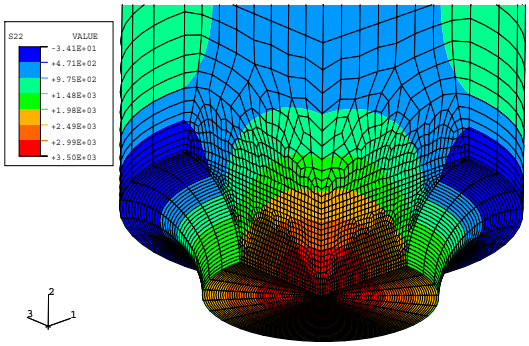

Figure 3: Axial stress in notched tensile specimen

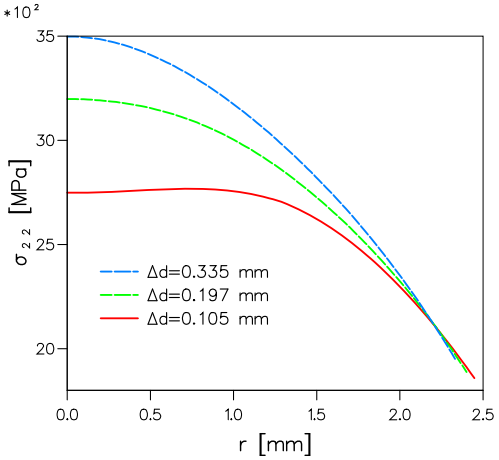

Figure 4: Axial stress distribution in the notched tensile specimen for three displacements at and below fracture

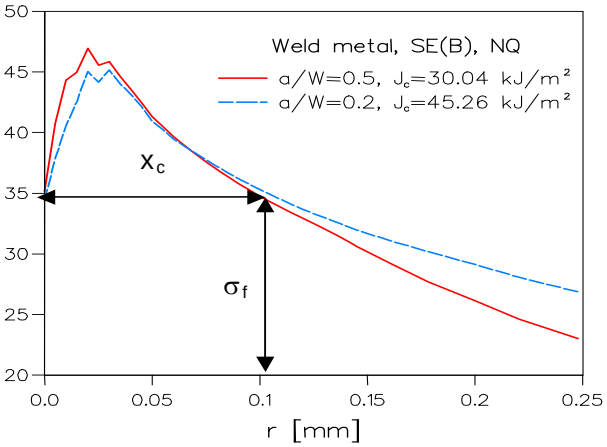

Figure 5: Evaluation of the Critical Distance x_c by the Numerical Simulation of SE(B) Specimens

Once the RKR model was qualified by the described procedure, any further specimen test or the final structural configuration could be investigated as shown in Figure 6 for SCT specimens.

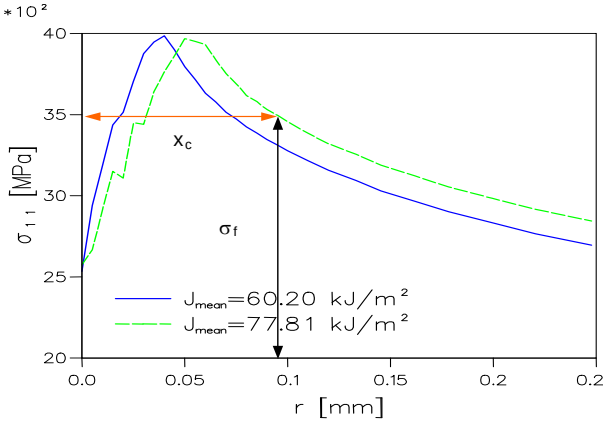

Figure 6: Stress Distribution at the Crack Tip for SCT Specimens

In addition to the local approach (RKR model), a two parameter fracture mechanics concept was applied to ductile material zones. A relation between the constraint

of different specimen or component geometries and the critical J-integral can be evaluated as shown in Figure 7.

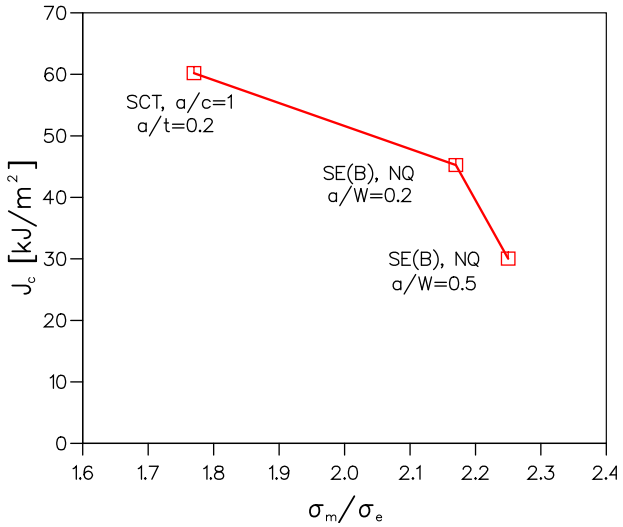

Figure 7: J-integral at failure for different specimens as a function of constraint

These two fracture prediction approaches then have been successfully applied to the sub-scale pressure vessel testing. Burst tests have been performed with several vessels (Figure 8) with surface and embedded cracks resulting from non-optimized welding at this stage of the program (Figure 9).

Figure 8: Sub-Scale Pressure Vessel after Burst Test

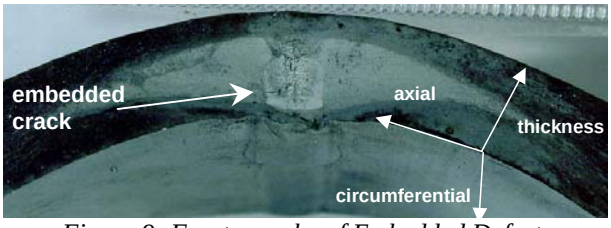

Figure 9: Fractography of Embedded Defect

The crack profiles were extended over different material zones and therefore both concepts (RKR and j-integral) were applied. The good agreement with the test results is shown in Table 3. In the case of the embedded deefect the larger difference between prediction and test results is explained by the complex geometry of the crack which was not completely modelled in the FE mesh.

Table 3: Experimental and Numerical Results of Burst Test Analysis

	Pressure at Burst	**Numerical Prediction**	
		J_c Concept	**RKR Model**
Vessel 1 *	93 MPa	81 MPa	78 MPa
Vessel 2 #	100 MPa	90 MPa	95 MPa
* embedded defect, # surface defect			

4.2 Ductile Fracture Simulation in AA 2219 Material at Cryogenc Conditions

The large cryogenic hydrogen and oxigen tanks of the ARIANE 5 main stage and upper stage are made of AA2219 aluminum alloy. The alloy shows high ductile fracture behaviour and failure prediction was performed with the Gurson damage model [14] for different material conditions, including welds. The Figure 10 shows the numerical simulation of a SE(B) specimen test results. The prediction of the void volume fraction allows the accurate prediction of crack initiation.

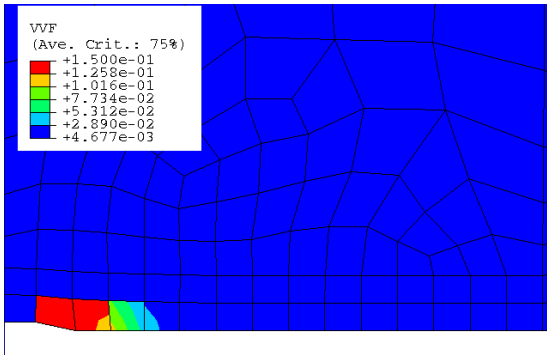

Figure 10: Numerical Simulation of the Void Volume Fraction in the SE(B) Specimen

The Figure 11 shows the good agreement between the numerical simulation and the test results.

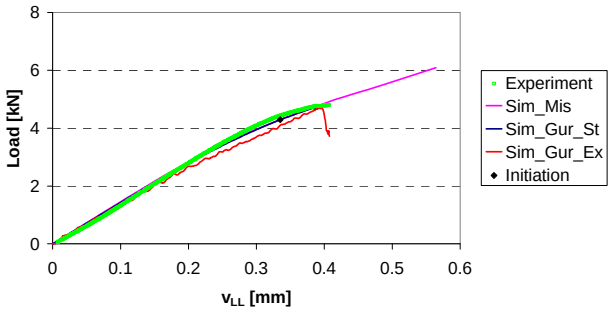

Figure 11: Load Displacement Behaviour of the SE(B) Specimen at -196 °C

Based on these results and large experience gained with the material and damage modeling, the fracture toughness of different crack configurations could be predicted as shown in Figure 12. The fracture toughness is shown versus triaxiality (mean normal stress / von Mises stress) for different surface crack configurations and the SE(B) specimen, thus identifying the conservatism of the standard specimen and further potential for structural assessment.

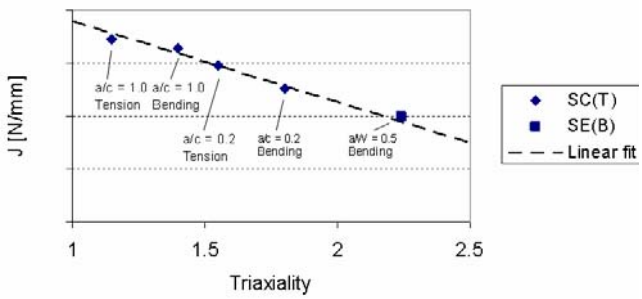

Figure 12: Relation between critical fracture toughness and stress triaxiality for the AA2219 Forging material at -196°C

4.3 Crack Initiation in AA2219 TIG Welds at Local Imperfections

The Gurson damage modelling has been further applied for the crack initiation at the fusion line of AA2219 TIG welds. The test result is shown in Figure 13, the numertrical simulation in Figure 14.

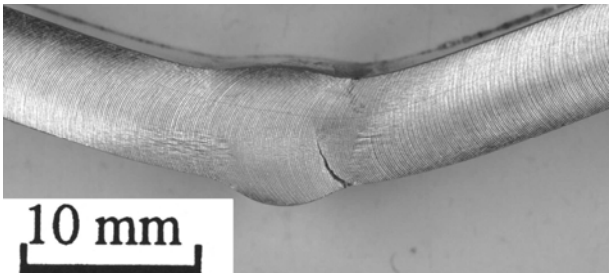

Figure 13: Bending Test of AA 2219 TIG Weld

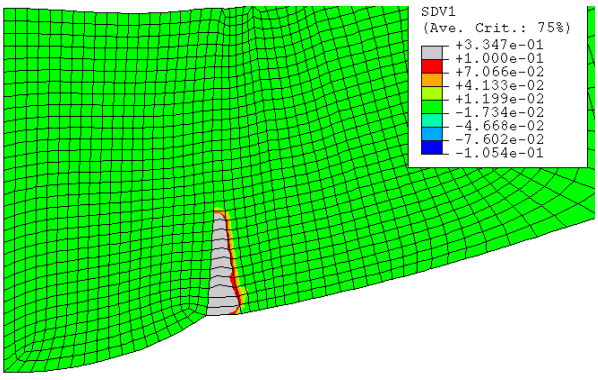

Figure 14: Damage Zone at the Fusion Line During Global Load Drop (Void Volume Fraction)

This kind of simulation allows the accurate prediction of local imperfections of TIG welds, where the assessment of local stress hot spots either by the application of notch factors or standard stress based FE analysis would give over-conservative results.

4.3 COPV BEHAVIOUR DURING AUTOFRETTAGE

High pressure vessels for spacecraft applications are in most cases made of metallic liners (titanium, INCONEL, stainless steels, aluminum) with composite overwrap. Autofrettage is performed to plastify the liner and result in compression stresses after unloading. The liner therefore shows high plastic strain and failure prediction has to be performed with non-linear methods.

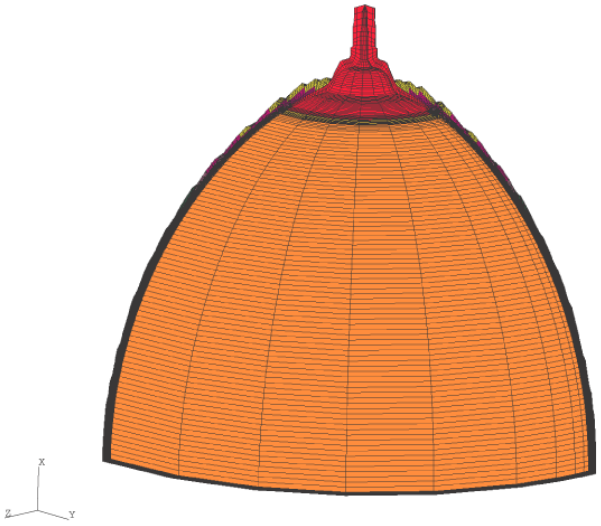

Figure 15:_ FE Mesh of theCOPV

Figure 16 shows details of the FE mesh of a COPV where a surface crack was investigated at the polar weld. Local weld imperfections were observed resulting in high local plasticity.

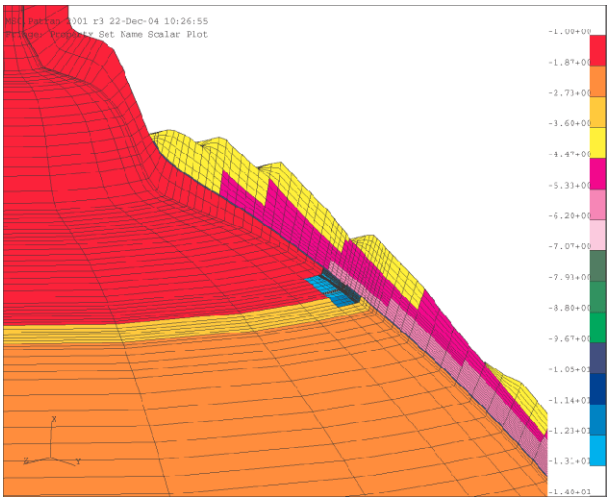

Figure 16: FE Mesh of the COPV with local Surface Crack

In this case even the application of non-linear based methods as SINTAP failed, as the analytical equations apply only for pure metallic crack cases. The COPV

however is shielded by the composite overwrap leading to displacement control even at plastified hot spots. This is demonstrated in Figure 17, where the j-integral prediction is shown versus pressure. The j-integral pressure relation remains linear over the complete pressure range although plastic strain up to 5 % appears. In a second step again Gurson simulation showed that no crack initiation occurred for a crack size, which is close to the inspection limits of the NDI.

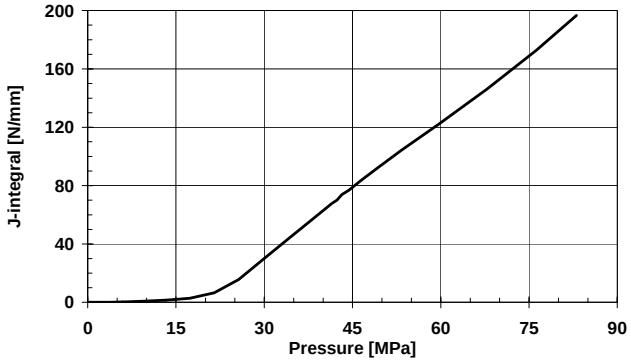

Figure 17: J-integral Dependence from COPV Inner Pressure

6. SUMMARY

The presented examples show the high potential of modern fracture mechanics methods based on damage mechanics modelling. Many phenomena as geometry dependence of fracture behaviour can now be explained and even quantified with those methods. It must however be pointed out that large experience is needed as these methods are highly sensitive both in parameter evaluation and numerical modelling. The here presented simulations have all been performed at FH-IWM Freiburg and I want especially thank D.Siegele, I.Varfolomeyev, D.Memhard, D.Sun and many others for their support.

Analytical prediction methods have not been referenced in this paper but may be found with detailed description and comparison with test results in [9,11].

5. REFERFENCES

NASA documents can be found at http://ntrs.nasa.gov/, ECSS standards can de downloaded from http://www.ecss.nl/.

[1] NASA-SP-8040
Fracture Control of Metallic Pressure Vessels

[2] NASA-CR-3957:
A Review of Fracture Mechanics Life Technology

[3] NASA 731-0005-83:
General Fracture Control Plan for Payloads using the Space Transportation System

[4] NASA-CR-4628:
Significant Issues in Proof Testing: A Critical Appraisal

[5] ECSS-E-ST-32-01C:
Space Engineering: Fracture Control

[6] Koçak et. al. (editors) 'FITNET Fitness-for-Service (FFS) – Procedure (Volume I) & Annex (Volume II)' Revision Mk8, January 2008,

[7] IWM-VERB, Version 8.0, Fraunhofer-Institut für Werkstoffmechanik, 2008

[8] Berger, C., J.G.Blauel, B.Pyttel and L.Hodulak, 'FKM Guideline – Fracture Mechanics Proof of Strength for Engineering Components', 2nd revised edition, 2004, VDMA Verlag GmbH, ISBN 3-8163-0496-6

[9] Windisch, M., Eisenmann, A., Albinger, J., Varfolomeyev, I., Memhard, D. Siegele,D.: Application of Analytical (SINTAP) and Damage Mechanics Based Numerical Simulation for the Assessment of (Plastically) Hot Spots in the ARIANE 5 Main Stage Tank Bulkheads, European Conference on Spacecraft Structures, Materials & Mechanical Testing 2005, Noordwijk, ESA SP-581

[10] Windisch, M., Clormann, U., Grunmach, G., Burget, W. ,Sun, D-Z.: Damage Tolerance Verification Concept of the Ariane 5 Booster Welding Interface, European Conference on Spacecraft Structures, Materials and Mechanical Testing, 2000 Noordwijk, ESASP-468, 2001., p.499

[11] Varfolomeyev, I., Hodulak, L., Siegele, D., Windisch, M.: Validation of the FITNET Analysis Procedure for the Assessment of ARIANE 5 Thin-Walled Components, Proceedings of FITNET 2006, International Conference on Fitness-for-Service, 17-19 May 2006, Amsterdam, The Netherlands

[12] Windisch, M., Sun, D-Z., Memhard, D., Siegele, D.: Defect Tolerance Assessment of ARIANE 5 Structures on the Basis of Damage Mechanics Material Modelling, Engineering Fracture Mechanics (2008)

[13] Ritchie, R.O., Knott, J.F., Rice, J.R., On the relationship between critical tensile stress and fracture toughness in mild steel, J. Mech. Phys. Solids, 21,1973, 395-410

[14] Gurson, A.L., Continuum Theory of Ductile Rupture by Void Nucleation and Growth: Part I – Yield Criteria and Flow Rules for Porous Ductile Media, J. Eng. Mater. Technology 99 (1977), 2-15